Journal of Hazardous Materials 192 (2011) 1555–1564

Contents lists available at ScienceDirect

Journal of Hazardous Materials

journal homepage: www.elsevier.com/locate/jhazmat

Comparative electrochemical treatments of two chlorinated aliphatic hydrocarbons. Time course of the main reaction by-products

Serena Randazzo[a,b], Onofrio Scialdone[b], Enric Brillas[a], Ignasi Sirés[a,*]

[a] Laboratori d'Electroquímica dels Materials i del Medi Ambient, Departament de Química Física, Facultat de Química, Universitat de Barcelona, Martí i Franquès 1-11, 08028 Barcelona, Spain

[b] Dipartimento di Ingegneria Chimica, Gestionale, Informatica e Meccanica, Università di Palermo, Viale delle Scienze, 90128 Palermo, Italy

ARTICLE INFO

Article history:
Received 7 April 2011
Received in revised form 10 June 2011
Accepted 27 June 2011
Available online 1 July 2011

Keywords:
1,2-Dichloroethane
Electrochemical water treatment technologies
Electro-Fenton
Organochlorinated pollutants
Reaction pathway
1,1,2,2-Tetrachloroethane

ABSTRACT

Acidic aqueous solutions of the chlorinated aliphatic hydrocarbons 1,2-dichloroethane (DCA) and 1,1,2,2-tetrachloroethane (TCA) have been treated by the electro-Fenton (EF) process. Bulk electrolyses were performed at constant current using a BDD anode and an air diffusion cathode able to generate H_2O_2 in situ, which reacts with added Fe^{2+} to yield •OH from Fenton's reaction. At 300 mA, almost total mineralization was achieved at 420 min for solutions containing 4 mM of either DCA or TCA. Comparative treatments without Fe^{2+} (anodic oxidation) or with a Pt anode led to a poorer mineralization. The better performance of the EF process with BDD is explained by the synergistic action of the oxidizing radicals, BDD(•OH) at the anode surface and •OH in the bulk, and the minimization of diffusional limitations. The decay of the initial pollutant accomplished with pseudo first-order kinetics. Chloroacetic and dichloroacetic acids were the major by-products during the degradation of DCA and TCA, respectively. Acetic, oxalic and formic acids were also identified. The proposed reaction pathways include oxidative and reductive (cathodic) dechlorination steps. Chlorine was released as Cl^-, being further oxidized to ClO_3^- and, mostly, to ClO_4^-, due to the action of the largely generated BDD(•OH) and •OH.

1. Introduction

The nowadays society finds it difficult to ensure the clean water supply because domestic, agricultural and industrial activities are responsible for introducing refractory organic pollutants into the water streams. Major attention is paid to contaminants with an aromatic structure because they tend to be more toxic than their aliphatic counterparts. However, serious concerns arise from the presence of chlorinated aliphatic hydrocarbons in waters. These compounds conjugate toxicity with high chemical stability, bioaccumulation and long-range diffusivity [1]. Chloroethanes are particularly ubiquitous in the industry and in household products, and their entry to the environment may entail potential risks for the living beings [2]. At present, the US Environmental Protection Agency is carrying out the Endocrine Disruptor Screening Program (EDSP), where 1,2-dichloroethane (DCA) and 1,1,2,2-tetrachloroethane (TCA) are considered as priorities for their potential effects on the endocrine system. DCA is also found in the list of priority substances drawn up by the European Commission [3].

To avoid the release of chloroethanes into the aqueous environment, powerful water treatment technologies such as the advanced oxidation processes (AOPs) must be applied in the wastewater treatment facilities. AOPs are based on the action of the •OH generated in situ to oxidize the biorecalcitrant organic matter [4,5]. Among them, electrochemical AOPs (EAOPs) such as anodic oxidation (AO) and electro-Fenton (EF) processes have gained much interest for the removal of organic compounds due to their outstanding technical characteristics [6–9]. Cañizares et al. [10–12] showed that the electrochemical degradation of organic pollutants using boron-doped diamond (BDD) anodes is more efficient than ozonation and Fenton oxidation, yielding higher removals at a competitive cost. In AO, the destruction of pollutants is mediated by hydroxyl radicals generated at the anode surface from water oxidation and its effectiveness depends dramatically on the anode material; BDD [13–23] and PbO_2 [17–19,24,25] have been widely employed for the destruction of dyes [18,20,21,25], pesticides [13–15,24,25], pharmaceutical residues [22,23] and industrial pollutants [16,19]. They exhibit much higher performance compared to classical anode materials due to the high oxidation ability of their physisorbed radicals (BDD(•OH) and PbO_2(•OH)) [26,27]. BDD is usually preferred because of its greater chemical and mechanical stability and higher current efficiency [28]. The interest on the EF process has also been growing [8]. In this EAOP, large amounts of •OH are produced in the bulk at acidic pH from Fenton's reaction

* Corresponding author. Tel.: +34 934021223; fax: +34 934021231.
E-mail address: i.sires@ub.edu (I. Sirés).

0304-3894/$ – see front matter © 2011 Elsevier B.V. All rights reserved.
doi:10.1016/j.jhazmat.2011.06.075

between cathodically electrogenerated H_2O_2 and added Fe^{2+}. The continuous electrogeneration of H_2O_2 enhances the efficacy and the environmental compatibility compared to Fenton oxidation [29]. The regeneration of Fe^{2+} from cathodic reduction of Fe^{3+} is also an advantage in EF process [8]. EF has also been applied to the degradation of dyes [25,30–36], pesticides [37,38], pharmaceutical residues [39–43] and industrial pollutants [44,45] at bench- and pilot-scale trials. All the reactions involved in the complex mechanisms of AO and EF have been thoroughly reviewed elsewhere [8,9].

There exist several works on the degradation of chlorinated aliphatic hydrocarbons by AOPs, although only a few focus on chloroethanes. Trichloroethylene, tetrachloroethylene and DCA were treated with Fenton's reagent [46–48], which for example led to 100% degradation of DCA but with only 78% total organic carbon (TOC) removal [48]. Based on these positive results, hybrid technologies that involve the Fenton's process, TiO_2 photocatalysis and/or O_3 have been proposed for the removal of these pollutants [49–53]. Regarding the electrochemical treatments, several reduction and oxidation alternatives have been tested for many organic halides, as recently reviewed by Rondinini and Vertova [1]. Electroreduction with a silver cathode yielded high abatements (>90%) for DCA and TCA [54]. However, this method mainly allows the efficient removal of the halogen(s) group(s), often ending in stable, toxic by-products [1,54]. Conversely, complete mineralization may be achieved with the alternative use of EAOPs. Thus, the AO of DCA gave high dissolved organic carbon (DOC) abatement with much higher current efficiencies using BDD than stainless steel, Pt, Au, Ebonex, stainless, Ti/IrO_2-Ta_2O_5 and PbO_2 anodes [55,56]. More recently, some of us proposed the coupling of AO with a BDD anode and electroreduction with a silver cathode for the treatment of DCA and TCA, thus taking advantage of the simultaneous cathodic and anodic reactions [57].

This article reports the degradation of acidic aqueous solutions of DCA and TCA under EF conditions, which benefits from the synergistic oxidation of hydroxyl radicals at the anode surface (BDD($^\bullet$OH)) and in the bulk ($^\bullet$OH). In contrast to all previous studies reporting the electrochemical treatment of chloroethanes at the electrode surfaces, the present work stresses the role of hydroxyl radicals co-generated in the bulk, aiming to minimize the usual diffusional limitations. Bulk electrolyses were performed at constant current with an air diffusion electrode (ADE) as the cathode to produce H_2O_2 and a BDD anode. The effect of various experimental parameters on the mineralization of single and multicomponent solutions was examined. The chromatographic identification and evolution of the main accumulated organic by-products allowed the proposal of original reaction pathways for DCA and TCA. In addition, the treatment of solutions containing a high concentration of initial Cl as DCA and TCA allowed the identification of the chlorinated species generated. Previous studies hypothesized that the low level of Cl^- in the solutions electrolyzed with a BDD anode were due to its oxidation to free chlorine (Cl_2) [58–60]. Other authors showed the additional generation of chlorinated oxoanions such as ClO_2^- and ClO_3^- when electrolyzing chloride salts [61,62], even suggesting the total transformation into ClO_4^- [28,63].

2. Experimental

2.1. Chemicals

DCA and TCA were reagent grade from Acros Organics (≥99%). Carboxylic acids used in high-performance liquid chromatography (HPLC) analyses and chlorinated inorganic salts used for ion chromatography (IC) were either reagent or analytical grade (≥98%) from Merck, Acros Organics, Fluka and Panreac. Sulfuric acid, anhydrous sodium sulfate and heptahydrated ferrous sulfate were analytical grade from Fluka and Merck. All solutions were prepared with ultra-pure water from a Millipore Milli-Q system with resistivity >18 MΩ cm.

2.2. Instruments and analytical procedures

Constant current electrolyses were performed with an AMEL 2053 potentiostat/galvanostat. The solution pH was measured with a Crison GLP 22 pH-meter. Colourimetric measurements were made with a Unicam UV4 Prisma double-beam UV/Vis spectrometer thermostated at 20 °C. The concentration of H_2O_2 was determined from the light absorption of the Ti(IV)–H_2O_2 coloured complex at λ = 408 nm. The mineralization of the solutions was assessed from the decay of their DOC, which was determined with ±2% accuracy on a Shimadzu VCSN TOC analyzer.

The decay of the concentration of DCA and TCA was followed by gas chromatography/mass spectrometry (GC/MS) using a Thermo Scientific TRACE GC Ultra gas chromatograph equipped with a Thermo Scientific TrisPlus autosampler in headspace mode and a DB-624 (60 m × 0.32 mm (i.d.) and 1.8 μm film thickness) capillary column from Agilent Technologies, coupled with a Thermo Scientific DSQII quadrupole mass spectrometer. The temperature ramp was 60 °C for 2 min, 8.0 °C min^{-1} up to 220 °C and hold time 5 min, and the temperature of the source was 200 °C. The identification was performed through comparison with pure standards. Isopropanol was employed as internal standard for quantification.

The time course of the carboxylic acid intermediates was followed by ion-exclusion HPLC using a Waters 600 chromatograph fitted with a Bio-Rad Aminex HPX 87H, 300 mm × 7.8 mm (i.d.), column at 35 °C, and coupled with a Waters 996 photodiode array detector selected at λ = 210 nm. A 4 mM H_2SO_4 solution was eluted at 0.6 mL min^{-1} as the mobile phase. The chlorinated inorganic anions were determined by IC using a Shimadzu 10 Avp HPLC coupled with a Shimadzu CDD 10 Avp conductivity detector. The liquid chromatograph was fitted with a Shim-Pack IC-A1S, 100 mm × 4.6 mm (i.d.), anion column at 40 °C, and the mobile phase was a solution with 2.4 mM tris(hydroxymethyl)aminomethane and 2.5 mM phthalic acid of pH 4.0 at 1.0 mL min^{-1}. All species were identified by comparison of their retention times (t_r) with those of pure standards.

2.3. Electrolytic systems

The electrolyses were conducted in a cylindrical, undivided, water-jacketed glass cell containing 130 mL of solution. A scheme of the electrolytic system used is shown in Fig. 1. The headspace above the solution was kept to a minimum to reduce the amount of possible volatile organic compounds (VOCs) in the gas phase. In addition, a condenser with circulating water at 10 ± 1 °C was used to prevent loss of VOCs. A copper cooling-finger was immersed in a water bath to reach the required temperature. The anode was usually a 3 cm^2 BDD film (1300 ppm of B, 1.33 μm thickness) deposited on single crystal p-type Si(1 0 0) wafers supplied by Adamant Technologies. Comparative experiments were performed using a 3 cm^2 Pt foil (99.99% purity) from SEMPSA. The cathode was always a 3 cm^2 carbon-PTFE ADE from E-TEK, which was fed with 0.35 L min^{-1} of compressed air to electrogenerate H_2O_2 from the two-electron reduction of O_2. The interelectrode gap was 1 cm.

The behaviour of single component solutions was assessed with 2 or 4 mM DCA or TCA and 0.035 M Na_2SO_4 at pH 3.0 and 10 ± 1 °C under a constant current between 100 and 450 mA. The EF treatments were performed using 0.5 mM Fe^{2+} as catalyst. Comparative AO experiments were made without Fe^{2+} and feeding the cathode with pure N_2. Multicomponent solutions containing both DCA and TCA were also degraded. All trials were performed under vigorous stirring with a magnetic bar to ensure a good mixing and repro-

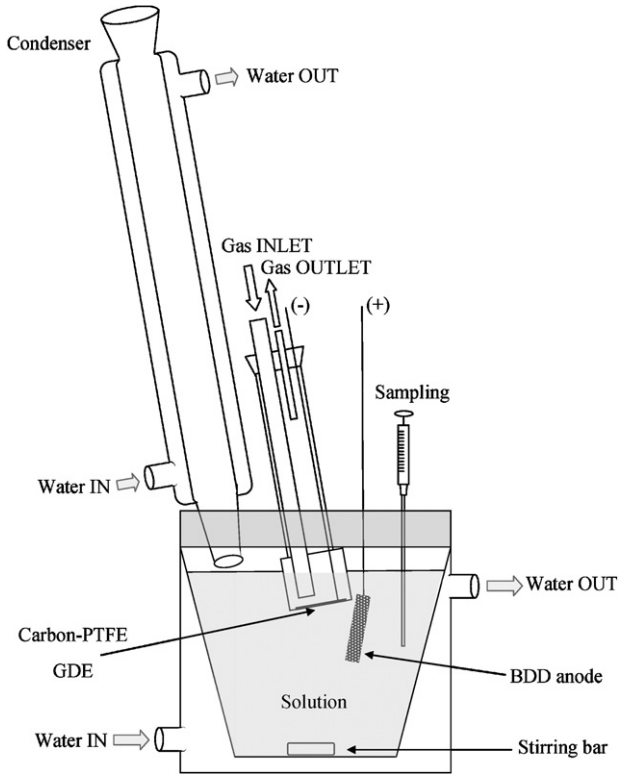

Fig. 1. Scheme of the experimental setup.

ducible mass transport conditions. The pH 3.0 was selected because it is the optimum value for Fenton's reaction [8].

3. Results and discussion

3.1. Mineralization of DCA and TCA solutions by EAOPs

Since the EF treatment is based on the H_2O_2 electrogeneration for the •OH production from Fenton's reaction, the first task was to ensure that the ADE cathode was able to produce enough H_2O_2 for the degradation of the organic matter. Fig. 2 shows the time course of this species during the electrolysis of several solutions with 0.035 M Na_2SO_4 at pH 3.0 and 10 °C in the BDD/ADE cell at 300 mA for 480 min. In the absence of Fe^{2+} and organics (AO conditions), H_2O_2 was gradually accumulated during the first 240 min,

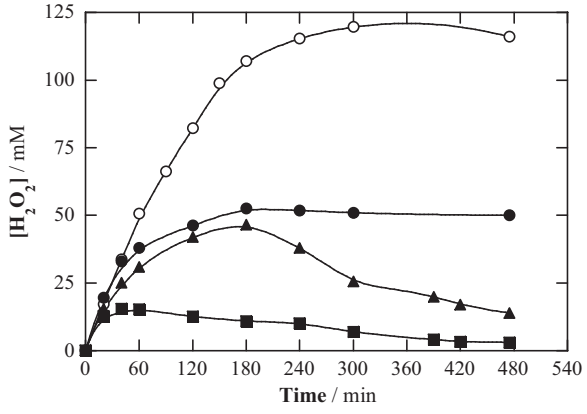

Fig. 2. Time course of accumulated H_2O_2 during the electrolysis of 130 mL of 0.035 M Na_2SO_4 solutions at pH 3.0, 300 mA and 10 °C using a BDD/ADE cell. Fe^{2+} concentration: (○) 0 mM and (●, ■, ▲) 0.5 mM; 1,2-dichloroethane (DCA) concentration: (○, ●) 0 mM, (▲) 2 mM and (■) 4 mM.

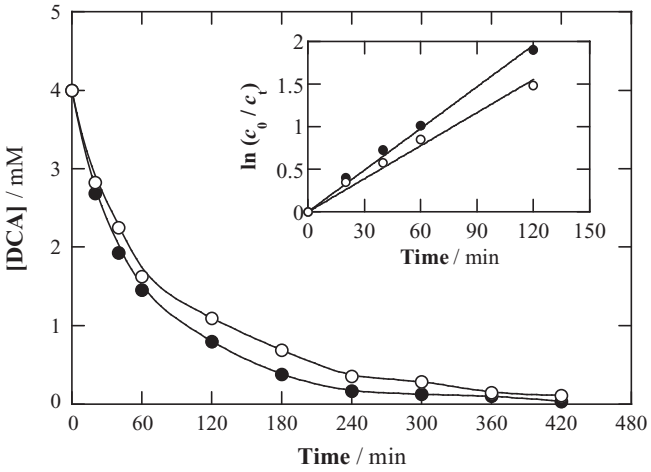

Fig. 3. DCA concentration vs electrolysis time during the degradation of 130 mL of 4 mM DCA in 0.035 M Na_2SO_4 at 300 mA, pH 3.0 and 10 °C using a BDD/ADE cell by (○) anodic oxidation (AO) with N_2 supply to the cathode and (●) electro-Fenton (EF) with 0.5 mM Fe^{2+}. The inset panel depicts the corresponding kinetic analysis assuming pseudo first-order reaction for DCA.

reaching a steady value of about 120 mM once the rate of H_2O_2 formation at the cathode became equal to its destruction rate at the cathode, at the anode and in the bulk.

When 0.5 mM Fe^{2+} was added (EF conditions), the steady state H_2O_2 concentration decreased to about 50 mM due to its rapid destruction mainly with Fe^{2+} through the classical Fenton's reaction yielding •OH [8,9]. Similar electrolyses carried out with 0.5 mM Fe^{2+} and 2 mM DCA yielded a lower maximum H_2O_2 concentration, which continuously decreased from 180 min. This behaviour is accounted for by a higher consumption of •OH for organic matter oxidation, which immediately enhances the H_2O_2 destruction by Fenton's reaction. The electrolysis of a 4 mM DCA solution produced even much lower H_2O_2 accumulation due to the larger amounts of •OH involved in the oxidation of organic compounds, thus accelerating the Fenton's reaction. The same trends were observed using TCA solutions (data not shown).

GC/MS was used to study the decay of the DCA and TCA concentration with time. Blank experiments with addition of commercial H_2O_2, but without current, demonstrated that DCA and TCA solutions were not degraded by this oxidant, indicating that generated hydroxyl radicals were the main species able to degrade both chloroethanes in AO and EF.

Fig. 3 shows the decay for 4 mM DCA solutions in 0.035 M Na_2SO_4 by AO (without Fe^{2+}, with N_2 supply to the cathode to prevent the H_2O_2 generation) and EF (0.5 mM Fe^{2+}, with air supply to the cathode) using the same BDD/ADE cell at 300 mA. A progressive destruction of DCA can be observed in AO by the main oxidative action of BDD(•OH), remaining 3% at 420 min. The quicker removal achieved in EF, with total disappearance in 420 min, confirms the higher oxidation power of this process. This can be explained by: (i) the higher concentration of hydroxyl radicals thanks to the simultaneity of two generation ways, BDD(•OH) at the anode and •OH in the bulk, and (ii) the minimization of the diffusional limitations that are inherent to the electrode processes such as AO. The inset of Fig. 3 depicts the excellent linear correlations, with $R^2 > 0.99$, obtained assuming pseudo first-order reaction between DCA and generated hydroxyl radicals. The apparent rate constant (k_{app}) determined for the experiments without and with Fe^{2+} were 0.013 and 0.016 min^{-1}, respectively, as expected for the quicker destruction in the EF process. A similar behaviour was found for TCA solutions (not shown).

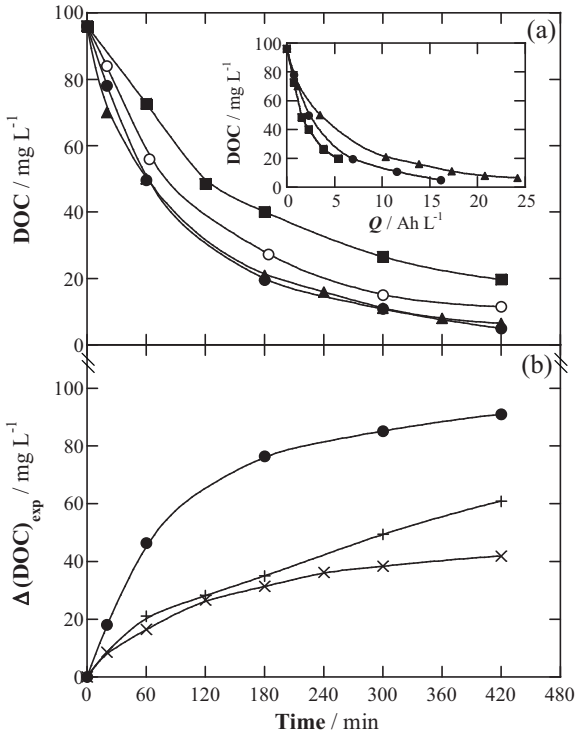

Fig. 4. (a) DOC abatement vs electrolysis time for treating 130 mL of 4 mM DCA in 0.035 M Na_2SO_4 at pH 3.0 and 10 °C using a BDD/ADE cell. (○) AO and (●, ■, ▲) EF with 0.5 mM Fe^{2+}. Current: (■) 100 mA, (○, ●) 300 mA and (▲) 450 mA. The inset panel shows the DOC removal vs specific charge for the EF trials. (b) $\Delta(DOC)_{exp}$ vs electrolysis time for the EF degradation of: (●) 4 mM and (×) 2 mM DCA in a BDD/ADE cell and (+) 4 mM DCA in a Pt/ADE cell. Current: 300 mA.

Fig. 4(a) shows the effect of several operating parameters on the DOC decay for the above 4 mM DCA (96.0 mg L^{-1} DOC) solutions using AO and EF. At 300 mA, a slower degradation was achieved by AO, with 91% DOC removal at 420 min, whereas almost total mineralization (>95% DOC decay) was reached by EF. Such enhancement is consistent with the larger production of hydroxyl radicals at the anode and in the bulk. This coupling leads to a conspicuous increase of the treatment efficiency because both anodic and cathodic currents contribute to the destruction of the organic matter. In fact, even the participation of some electroreduction reactions cannot be discarded until the intermediates are analysed, although such reactions are expected to be much less significant compared to the BDD(•OH)/•OH-mediated reactions. Fig. 4(a) also shows acceleration in DOC abatement with increasing current for the EF treatment. The degradation rate was much lower at 100 mA due to the lower production rate of •OH and BDD(•OH), only achieving 80% mineralization at the end of the electrolysis. The faster oxidation of H_2O, electrogeneration of H_2O_2 and cathodic regeneration of Fe^{2+} at 300 mA largely contributes to the significant acceleration of the degradation process. However, the enhancement obtained from 300 to 450 mA was not as remarkable as that produced from 100 to 300 mA, suggesting a greater limitation by mass transport phenomena at high current, i.e., the oxidation rate becomes mainly controlled by the transport of oxygen and iron ions toward the cathode and organic compounds toward the anode. The inset panel of Fig. 4(a) shows that an increase in the applied current, from 100 to 450 mA, causes higher specific charge consumption for attaining a given DOC value (i.e., a lower current efficiency). This is due to the increasing extent of the parasitic reactions such as O_2 evolution, which do not invest the hydroxyl radicals to oxidize the organic matter, thereby leading to the progressive waste of the supplied current.

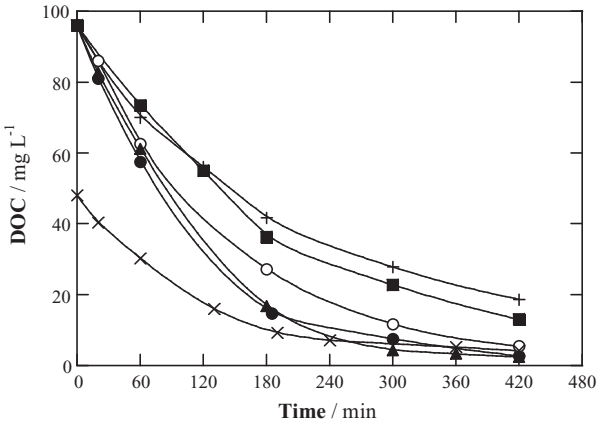

Fig. 5. DOC removal with electrolysis time for the treatment of 1,1,2,2-tetrachloroethane (TCA) solutions under the same conditions of Fig. 4.

Fig. 4(b) presents the evolution of $\Delta(DOC)_{exp}$ for the above EF degradation of 4 mM DCA at 300 mA compared to 2 mM DCA (48.0 mg L^{-1} DOC). A larger amount of DOC was removed when treating 4 mM DCA at any time and at the end of electrolysis, 42 and 91 mg L^{-1} of DOC were removed for 2 and 4 mM DCA, respectively. This means that at a higher pollutant concentration the EF process proceeds very well; a smaller fraction of hydroxyl radicals is wasted in parasitic reactions (e.g., reactions between the radicals and H_2O_2 or iron species, as well as self-dimerisation to H_2O_2) because they interact with a larger number of organic molecules that are available. As a result, a more efficient process was obtained for 4 mM DCA. Fig. 4(b) also depicts the comparison of the EF treatment of 4 mM DCA in the BDD/ADE and Pt/ADE cells at 300 mA, with applied potentials of 28–30 and 20–22 V, respectively. As observed, the latter cell yielded a much poorer mineralization, with only 61% DOC removal at 420 min. This confirms the importance of the oxidation process at the BDD anode, which becomes a fundamental synergistic contribution to the oxidation in the bulk.

Fig. 5 depicts the effect of the same operating parameters on the mineralization of similar TCA solutions using the BDD/ADE and Pt/ADE cells. The conclusions drawn are analogous to those of Fig. 4, although the degradation rate from 120 min becomes slightly higher than that of DCA, probably due to the formation of more easily oxidizable by-products. Thus, the solutions of 4 mM TCA were completely mineralized by EF with BDD at 300 and 450 mA, whereas AO with BDD and EF with Pt led to 94% and 80% DOC removal, respectively.

3.2. Time course of the main reaction by-products

GC/MS analysis of the above electrolyzed solutions did not show any other chloroalkane or chloroalkene as organic by-product. Since hydroxylated compounds are formed from BDD(•OH)/•OH-mediated oxidation [8], the generated short-chain carboxylic acids were analyzed by ion-exclusion HPLC. Figs. 6 and 7 show the time course of acids detected during the treatment of DCA and TCA solutions under the conditions of Figs. 4 and 5, respectively. These by-products are always accumulated in the first stage of all treatments because their generation from the cleavage of the parent molecules, whose high initial concentration causes the consumption of most of the hydroxyl radicals, predominates over their destruction, and after reaching a maximum concentration they are progressively converted into other by-products and/or $CO_2 + H_2O$.

Four acids were formed for DCA: chloroacetic (t_r = 14.7 min) and acetic (t_r = 14.9 min) displayed two partially overlapped peaks in the chromatograms, whereas the peaks for oxalic (t_r = 6.9 min) and formic (t_r = 13.7 min) appeared isolated. Since the same calibra-

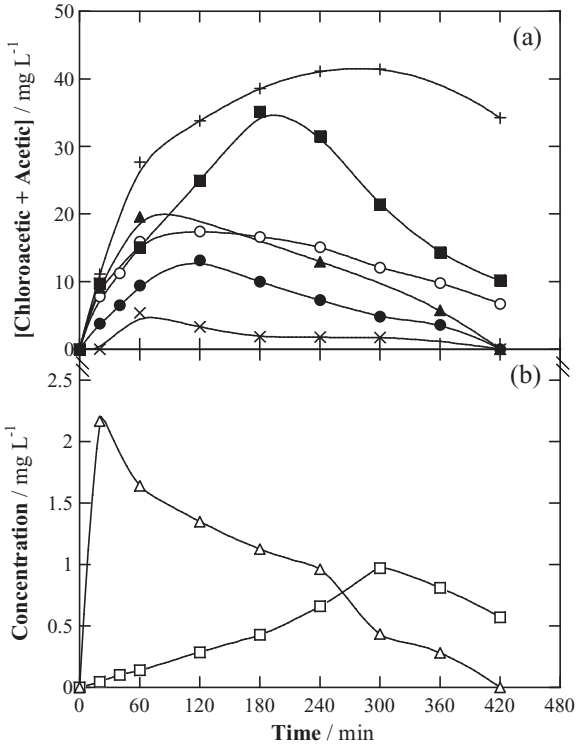

Fig. 6. (a) Time course of the concentration of chloroacetic + acetic acids detected during the mineralization of DCA under the conditions of Fig. 4. (b) Evolution of (□) oxalic and (△) formic acids during the EF degradation of 4 mM DCA in a BDD/ADE cell at 300 mA.

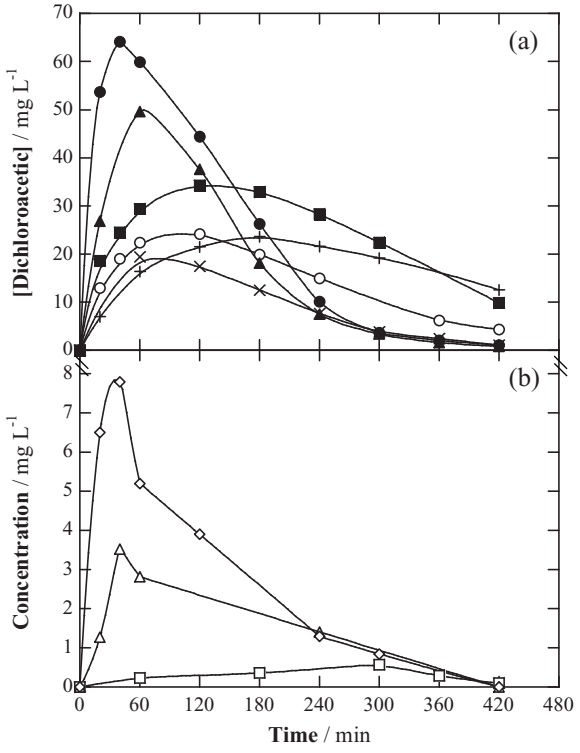

Fig. 7. (a) Evolution of dichloroacetic acid found during the degradation of TCA in the same conditions as in Fig. 5. (b) Time course of (◊) chloroacetic + acetic, (□) oxalic and (△) formic acids during the EF treatment of 4 mM TCA in a BDD/ADE cell at 300 mA.

tion curve was found for chloroacetic and acetic acids, their sum is plotted in Fig. 6(a) for all experiments. As can be seen, EF with BDD at 300 mA leads to a maximum of 12 mg L^{-1} for this couple at 120 min, whereupon they are rapidly destroyed up to reaching total destruction at 420 min. Under these conditions, Fig. 6(b) shows lower concentrations for formic and oxalic acids, the latter being more persistent and remaining in the final electrolyzed solution. The importance of chloroacetic + acetic acids as the major by-products is confirmed for the trials at 100 and 450 mA. Fig. 6(a) also depicts that they undergo higher accumulation in AO due to the absence of •OH in the bulk, although EF with Pt yields the largest accumulation, reaching >40 mg L^{-1} and being very slowly degraded. This corroborates the important role of hydroxyl radicals generated at the anode surface in the degradation process, BDD(•OH) being much more active than Pt(•OH) and •OH in the bulk regarding the destruction of refractory compounds. Table 1 summarizes the DOC values determined at 60 and 420 min for all experiments, as well as the equivalent carbon content corresponding to the concentration found for carboxylic acids. It can be seen that the contribution of oxalic and formic acids to DOC is always much lower than that of chloroacetic + acetic acids.

In the case of TCA, the chromatograms displayed the peaks related to the same four acids plus dichloroacetic acid (t_r = 8.1 min). As shown in Fig. 7(a) and in Table 1, dichloroacetic acid is always the major by-product, reaching >60 mg L^{-1} in EF with BDD at 300 mA. However, it is slightly less persistent than chloroacetic + acetic acids, since it undergoes some degradation in EF with Pt anode, but can be considered a refractory compound like chloroacetic shown above. This explains the higher DOC removal found for TCA (80%) compared to DCA (61%) in EF with the Pt/ADE cell at 300 mA, as well as the slightly higher degradation rate of TCA solutions from 120 min of electrolysis (Figs. 4 and 5). Fig. 7(b) shows the trends of the other acids, which were totally removed.

It is important to notice that (mono)chloroacetic and dichloroacetic acid are typically formed during the disinfection of waters by chlorination, and their control is mandatory due to their potential carcinogenic and mutagenic effects [53]. Our findings for EF with Pt completely agree with others reported elsewhere for the Fenton treatment of these haloacetic acids [49,51,52]. For example, Nogueira et al. [51] and Lee et al. [52] found that dichloroacetic is very slowly and only partially oxidized by •OH generated from Fenton's reaction. Similarly, we have found that •OH and Pt(•OH) yield poor results for these acids and/or their simultaneously formed iron complexes. In contrast, it is very worth remarking that EF with BDD is able to completely destroy them, which confirms the importance of the synergistic action of BDD(•OH). As will be discussed in Section 3.4, the BDD surface and/or the BDD(•OH) are fundamental to allow the oxidation of other refractory species such as acetic acid and Fe(III)-oxalate complexes [8].

Mixtures containing 2 mM DCA and 2 mM TCA were treated by EF with BDD at 300 mA to verify the decontamination of multicomponent solutions. As depicted in Fig. 8, the almost complete mineralization of solutions was achieved at 600 min. The abovementioned five carboxylic acids were also identified in this experiment, being confirmed that dichloroacetic and chloroacetic + acetic are the major by-products, as shown in the inset panel of Fig. 8 and in Table 1.

3.3. Fate of the chlorine contained in DCA and TCA

Ion chromatography revealed the formation of Cl^-, ClO_3^- and ClO_4^- ions during all electrolyses. The percentage of total Cl in these ions, along with their distribution, after 60 and 420 min of all experiments is summarized in Table 1. Fig. 9 exemplifies the evolution of these ions for the EF treatment of 4 mM DCA or TCA with BDD at 300 mA. Fig. 9(a) shows that chlorine is primarily released as Cl^-

Table 1
Chlorine and carbon amounts contained in the chlorinated ions and carboxylic acids determined as the reaction by-products during the electrolyses of DCA, TCA, and DCA + TCA at pH 3.0 and 10 °C.

Anode	[DCA] (mM)	[TCA] (mM)	DOC (mg L^{-1})	[Fe^{2+}] (mM)	I (mA)	t (min)	Cl content from different sources (%)[1,2]			Carbon content from different sources (mg L^{-1})[1,2,3,4,5]				
							Sum of chlorinated ions (Cl^-; ClO_3^-; ClO_4^-)	DCAA	MCAA	DOC	OXA	DCAA	FOR	MCAA + ACE
BDD	4	–	96.0	–	300	60	50.9 (34.6; 47.1; 18.3)	–	0–2.1	55.0	0.06	–	0.3	4.0–6.4
						420	92.6 (5.8; 23.3; 70.9)	–	0–0.9	8.1	0.02	–	0.1	1.7–2.7
		–		0.5		60	58.7 (53.5; 35.8; 10.7)	–	0–1.2	49.6	0.04	–	0.4	2.4–3.8
						420	97.0 (2.9; 6.9; 90.2)	–	0	5.0	0.2	–	0	0
		–			100	60	29.8 (72.4; 24.5; 3.1)	–	0–2.0	72.6	0.06	–	0.4	3.8–6.0
						420	82.2 (16.2; 52.8; 31.0)	–	0–1.3	19.7	0.2	–	0.2	2.6–4.1
		–			450	60	52.4 (44.3; 34.1; 21.6)	–	0–2.6	50.0	0.03	–	0.7	5.0–7.8
						420	92.8 (3.5; 10.1; 86.4)	–	0	6.5	0.1	–	0	0
	2	–	48.0		300	60	50.0 (45.0; 37.0; 18.0)	–	0–1.4	31.6	0.06	–	0	1.4–2.1
						420	92.6 (13.5; 21.7; 64.8)	–	0	6.1	0.03	–	0	0
	–	4	96.0	–	300	60	28.9 (47.0; 22.6; 30.4)	2.2	0–0.4	62.5	0.01	4.2	0.9	1.4–2.2
						420	77.1 (4.5; 7.2; 88.3)	0.4	0–0.02	5.5	0	0.8	0.4	0.08–0.1
	–			0.5		60	38.1 (55.3; 13.1; 31.6)	5.8	0–0.3	57.5	0.06	11.1	0.7	1.3–2.1
						420	97.8 (5.4; 8.3; 86.3)	0.1	0	2.7	0.03	0.2	0	0
	–				100	60	23.1 (69.0; 26.4; 4.61)	2.8	0–0.02	73.4	0.01	5.5	0.4	0.08–0.1
						420	77.3 (12.9; 38.5; 48.5)	1.0	0–0.04	13.1	0	1.8	0.2	0.2–0.3
	–				450	60	53.3 (43.5; 16.0; 40.5)	4.8	0–0.2	61.1	0.03	9.2	0.8	0.6–1.0
						420	89.5 (2.1; 4.2; 93.7)	0.08	0	2.4	0	0.2	0	0
	–	2	48.0		300	60	41.4 (41.3; 12.3; 46.4)	3.8	0	30.2	0	3.6	1.0	0
						420	97.8 (3.2; 4.5; 92.3)	0.2	0	4.2	0	0.2	0	0
	2	2	96.0	0.5	300	60	51.9 (44.7; 33.5; 21.8)	1.2	0–0.8	65.2	0.03	1.8	0.4	2.3–3.6
						420	91.8 (2.8; 5.6; 91.6)	0.1	0–0.1	9.5	0	0.1	0.06	0.4–0.6
Pt	4	–	96.0	0.5	300	60	26.4 (77.3; 12.9; 9.8)	–	0–3.7	74.9	0.01	–	1.4	7.0–11.1
						420	71.2 (21.0; 31.9; 47.0)	–	0–4.5	35.1	0.02	–	0.5	8.7–13.7
	–	4	96.0	0.5	300	60	25.2 (70.6; 7.6; 21.8)	1.6	0–0.1	70.0	0.01	3.1	0.2	0.5–0.8
						420	75.8 (10.3; 16.4; 73.3)	1.2	0–0.06	18.7	0.01	2.3	0.2	0.3–0.4

Carboxylic acid: [1]DCAA: Dichloroacetic; [2]MCAA: Chloroacetic; [3]OXA: Oxalic; [4]FOR: Formic; [5]ACE: Acetic.

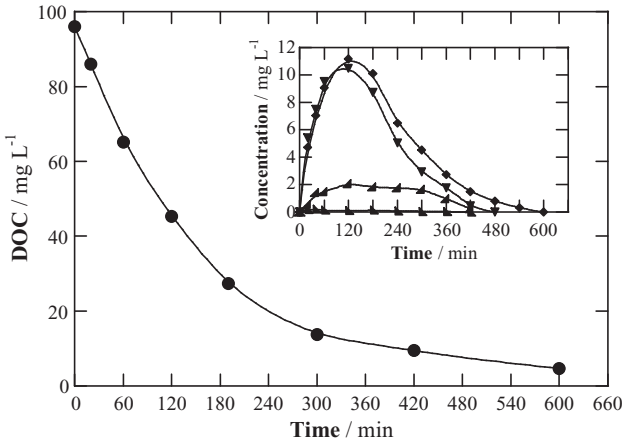

Fig. 8. DOC removal with electrolysis time for 130 mL of a solution with 2 mM DCA and 2 mM TCA in 0.035 M Na_2SO_4 with 0.5 mM Fe^{2+} at pH 3.0, 300 mA and 10 °C by EF using a BDD/ADE cell. The inset panel presents the concentration change for the short-chain carboxylic acids accumulated: (♦) chloroacetic + acetic, (▼) dichloroacetic, (◣) oxalic and (◢) formic.

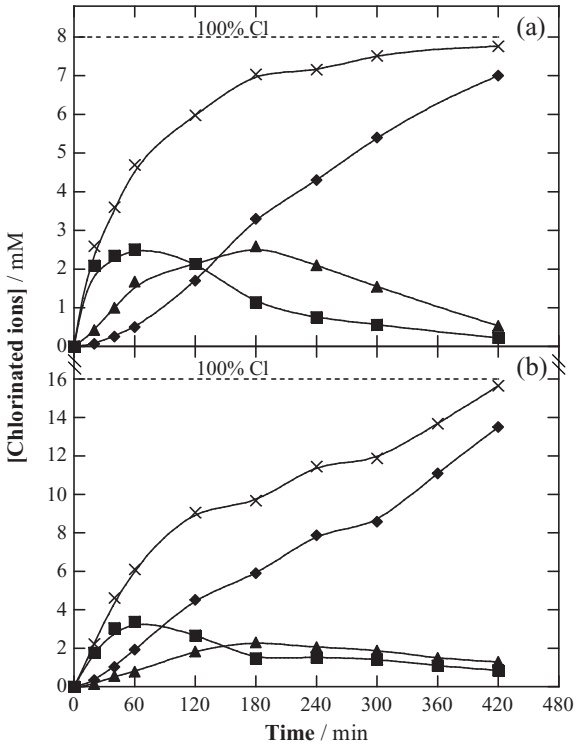

Fig. 9. Evolution of the concentration of the chlorinated ions released during the EF degradation of (a) 4 mM DCA and (b) 4 mM TCA in a BDD/ADE cell at 300 mA. Ion: (■) Cl^-, (▲) ClO_3^-, (♦) ClO_4^- and (×) sum of the three ions.

from DCA, reaching a 31.4% of initial Cl at 60 min. At this time, ClO_3^- and ClO_4^- are present to a smaller extent (27.3% of initial Cl) and the remaining DCA and chloroacetic acid contain 36.6% (Fig. 3) and 1.2% (Fig. 6(a)) of initial Cl. With increasing electrolysis time, the amount of Cl^- decreased, whereas that of ClO_3^- and ClO_4^- raised. At 420 min, the chlorinated ions accounted for 97.0% of initial Cl, being 87.5% as ClO_4^-, which is the least reactive oxidant among the chlorinated oxoanions due to its close shell structure. A similar behaviour can be observed in Fig. 9(b) for TCA, with 84.4% of initial Cl as ClO_4^- at 420 min. Data of Table 1 confirm that higher currents favor the formation of ClO_4^- in EF with BDD. Moreover, the use of BDD instead of Pt leads to a more pronounced accumulation of ClO_4^-.

Our results agree with recent findings reporting the formation of ClO_3^- [61] and even its total transformation into ClO_4^- for the electrolysis of inorganic chloride salts with BDD [28,63]. It can be assumed that Cl^- ions released during DCA and TCA degradation are oxidized at the BDD surface to active chlorine (Cl_2), being kinetically favored by the high overpotential of oxygen evolution at BDD [61]. Then, Cl_2 reacts with water in the bulk to yield HClO that is consecutively transformed into ClO_3^- and ClO_4^- [60]. These latter reactions are expected to occur under the action of •OH and BDD(•OH) [28,61,63]. The large amounts of both hydroxyl radicals produced in EF with BDD at high current can thus explain the almost total transformation into ClO_4^-. Similarly to what is reported for BDD, the AO mechanism to form ClO_4^- at Pt involves the Pt(•OH) [64]. Since this radical is much less active than BDD(•OH), one can infer that the main contribution to the formation of ClO_4^- in EF with Pt comes from the oxidation by •OH in the bulk.

3.4. Proposed pathways for DCA and TCA mineralization

From the identified by-products, the reaction pathways for the mineralization of DCA and TCA by EAOPs are proposed in Fig. 10(a) and (b), respectively. These sequences involve both reductive and oxidative dechlorination steps. Note that all the kinds of generated hydroxyl radicals are represented as •OH and all the acids are given in their uncomplexed forms for the sake of simplicity, although their complexes with iron species are always present.

Pathway A in Fig. 10(a) involves the oxidative dechlorination of DCA to form chloroacetic acid, which is the major degradative route according to the concentrations determined for the different by-products (see Fig. 6). Independent electrolyses performed for this acid showed that it is directly converted into CO_2. Pathway B is similar to A, but corresponds to the total oxidative dechlorination of DCA to oxalic acid. While the oxidation of most carboxylic acids mainly occurs at the anode surface, in the case of oxalic there exists a competition between the direct charge transfer and the hydroxyl radical-mediated oxidation [65–67]. In contrast, the Fe(III)-carboxylate complexes tend to be more rapidly destroyed by •OH in the bulk, but the Fe(III)-oxalate complexes are not oxidized in the bulk and their reaction with BDD(•OH) is also strongly inhibited, only being very slowly destroyed by direct charge transfer at the BDD surface [8,68]. Finally, pathway C is a mixture of oxidative and reductive dechlorination that allows justifying the formation of acetic acid. Note that the mechanism for the electroreduction of an R–X bond (R = hydrocarbon chain, X = F, Cl, Br, I) based on the Marcus theory explains the one-electron transfer leading to RH and X^- [1]. Recently, Kapalka et al. [69] demonstrated that in AO with BDD, acetic acid only reacts with BDD(•OH), although its adsorption on the BDD surface causes the autoinhibition of the oxidation. However, in EF with BDD, acetic acid and its Fe(III) complexes can be totally removed thanks to the contribution of •OH in the bulk. Therefore, acetic acid is oxidized to oxalic and formic acids which are directly transformed into CO_2 [67].

Fig. 10(b) includes analogous sequences for TCA mineralization. Pathway A' is an oxidative dechlorination yielding dichloroacetic acid, which was confirmed to be directly oxidized to CO_2. This is the main pathway for TCA. Pathway B′ leads to oxalic acid like in pathway B. Pathway C′ involves the oxidative and reductive dechlorination steps like in pathway C to yield acetic acid. Finally, pathway D′ is an alternative to C′ with only one reductive dechlorination step to generate chloroacetic acid, which is directly converted into CO_2 as in Pathway A.

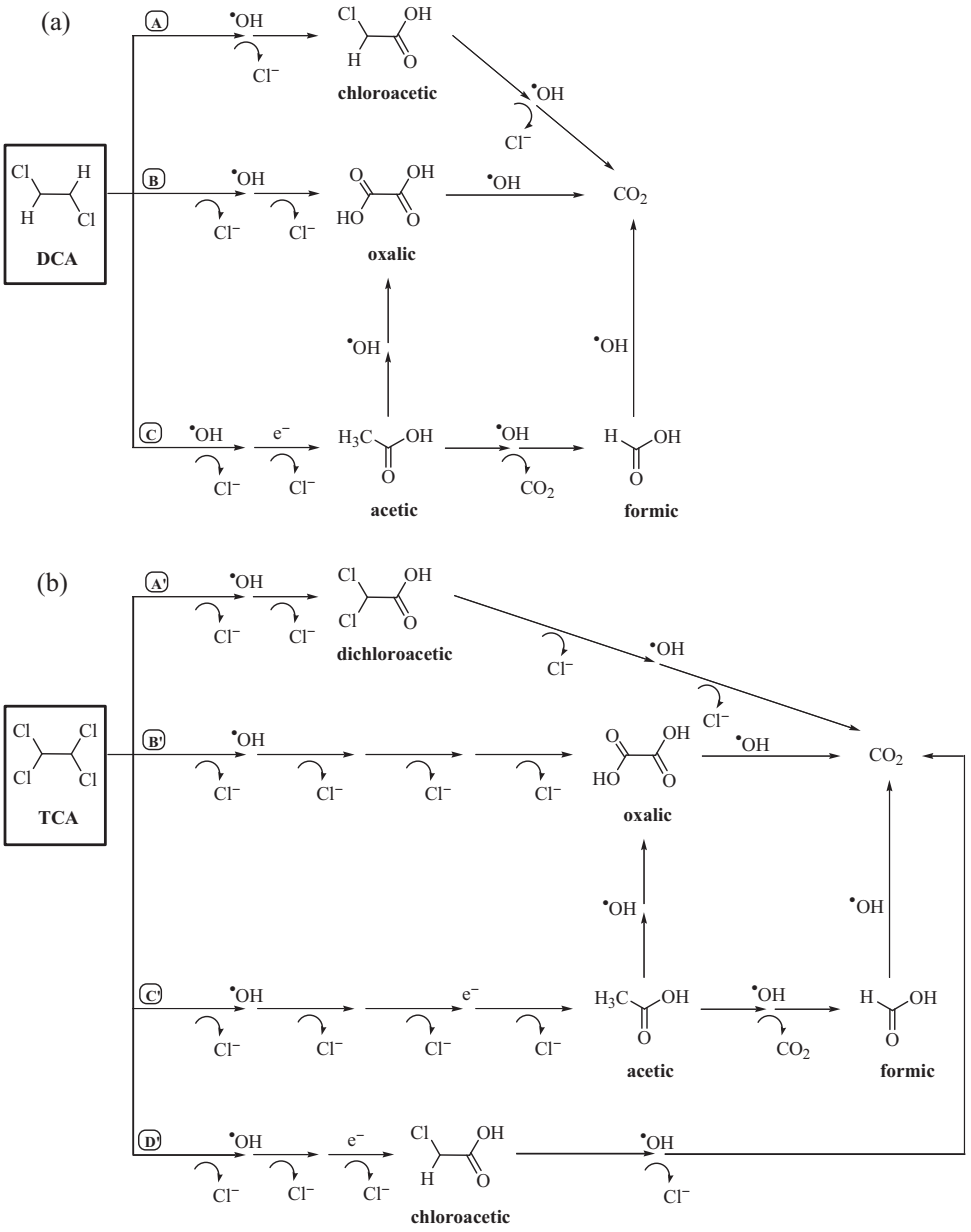

Fig. 10. Proposed reaction pathways for the mineralization of acidic aqueous solutions of: (a) DCA and (b) TCA by EAOPs.

4. Conclusions

It has been proven that EF with a BDD/ADE cell is a very effective technology for the decontamination of single and multicomponent DCA and TCA solutions. The determination of the time course of the main reaction by-products allowed clarifying the electrochemical degradation routes. Reductive (cathodic) and oxidative dechlorination steps contributed to the complete mineralization of DCA and TCA. However, as expected from the low electrocatalytic activity of the ADE to promote the electroreduction of the C-Cl bond, the oxidative dechlorination mediated by •OH and BDD(•OH) had the pre-eminent role, yielding the quicker destruction of major hardly oxidizable by-products such as chloroacetic, dichloroacetic and acetic acids. A slightly lower mineralization rate was observed for DCA compared to TCA because of the harder oxidation of chloroacetic compared to dichloroacetic. The BDD surface and the BDD(•OH) are then fundamental to achieve the complete destruction of the haloacetic acids, which otherwise can only be partially and slowly mineralized by •OH formed from Fenton's reaction. The action of •OH and BDD(•OH) was also fundamental to convert the released Cl^- into ClO_3^- and ClO_4^-, with production of more than 90% of the latter ion at high current.

Acknowledgements

Financial support from MICINN (Ministerio de Ciencia e Innovación, Spain) under project CTQ2010-16164/BQU, co-financed by FEDER funds, and from Università di Palermo is acknowledged.

References

[1] S. Rondinini, A. Vertova, Electroreduction of halogenated organic compounds, in: C. Comninellis, G. Chen (Eds.), Electrochemistry for the Environment, Springer Science + Business Media, New York, 2010, pp. 279–306.
[2] Chlorinated hydrocarbons, in: Ullmann's Encyclopedia of Industrial Chemistry, Wiley-VCH Verlag GmbH & Co. KGaAed, 2002 (electronic edition).

[3] European Commission, Identification of Priority Hazardous Substances under the Water Framework Directive, Directorate-General Environment, 2000.
[4] J.J. Pignatello, E. Oliveros, A. MacKay, Advanced oxidation processes for organic contaminant destruction based on the Fenton reaction and related chemistry, Crit. Rev. Environ. Sci. Technol. 36 (2006) 1–84.
[5] M. Klavarioti, D. Mantzavinos, D. Kassinos, Removal of residual pharmaceuticals from aqueous systems by advanced oxidation processes, Environ. Int. 35 (2009) 402–417.
[6] C.A. Martínez-Huitle, S. Ferro, Electrochemical oxidation of organic pollutants for the wastewater treatment: direct and indirect processes, Chem. Soc. Rev. 35 (2006) 1324–1340.
[7] A. Anglada, A. Urtiaga, I. Ortiz, Contributions of electrochemical oxidation to waste-water treatment: fundamentals and review of applications, J. Chem. Technol. Biotechnol. 84 (2009) 1747–1755.
[8] E. Brillas, I. Sirés, M.A. Oturan, Electro-Fenton process and related electrochemical technologies based on Fenton's reaction chemistry, Chem. Rev. 109 (2009) 6570–6631.
[9] M. Panizza, G. Cerisola, Direct and mediated anodic oxidation of organic pollutants, Chem. Rev. 109 (2009) 6541–6569.
[10] P. Cañizares, R. Paz, C. Sáez, M.A. Rodrigo, Electrochemical oxidation of alcohols and carboxylic acids with diamond anodes. A comparison with other advanced oxidation processes, Electrochim. Acta 53 (2008) 2144–2153.
[11] A. Beteta, P. Cañizares, M.A. Rodrigo, L. Rodríguez, C. Sáez, Treatment of door-manufacturing factories wastewaters using CDEO and other AOPs. A comparison, J. Hazard. Mater. 168 (2009) 358–363.
[12] P. Cañizares, R. Paz, C. Sáez, M.A. Rodrigo, Costs of the electrochemical oxidation of wastewaters: a comparison with ozonation and Fenton oxidation processes, J. Environ. Manage. 90 (2009) 410–420.
[13] C. Flox, J.A. Garrido, R.M. Rodríguez, F. Centellas, P.L. Cabot, C. Arias, E. Brillas, Degradation of 4,6-dinitro-*o*-cresol from water by anodic oxidation with a boron-doped diamond electrode, Electrochim. Acta 50 (2005) 3685–3692.
[14] A.M. Polcaro, A. Vacca, M. Mascia, S. Palmas, Oxidation at boron doped diamond electrodes: an effective method to mineralise triazines, Electrochim. Acta 50 (2005) 1841–1847.
[15] C. Flox, P.L. Cabot, F. Centellas, J.A. Garrido, R.M. Rodríguez, C. Arias, E. Brillas, Electrochemical combustion of herbicide mecoprop in aqueous medium using a flow reactor with a boron-doped diamond anode, Chemosphere 64 (2006) 892–902.
[16] M. Panizza, G. Cerisola, Biological and electrochemical oxidation of naphthalene sulfonates in a contaminated site leachate, J. Chem. Technol. Biotechnol. 81 (2006) 225–232.
[17] I. Sirés, E. Brillas, G. Cerisola, M. Panizza, Comparative depollution of mecoprop aqueous solutions by electrochemical incineration using BDD and PbO_2 as high oxidation power anodes, J. Electroanal. Chem. 613 (2008) 151–159.
[18] L.S. Andrade, T.T. Tasso, D.L. da Silva, R.C. Rocha-Filho, N. Bocchi, S.R. Biaggio, On the performances of lead dioxide and boron-doped diamond electrodes in the anodic oxidation of simulated wastewater containing the Reactive Orange 16 dye, Electrochim. Acta 54 (2009) 2024–2030.
[19] C. Flox, C. Arias, E. Brillas, A. Savall, K. Groenen-Serrano, Electrochemical incineration of cresols: a comparative study between PbO_2 and boron-doped diamond anodes, Chemosphere 74 (2009) 1340–1347.
[20] M. Hamza, R. Abdelhedi, E. Brillas, I. Sirés, Comparative electrochemical degradation of the triphenylmethane dye Methyl Violet with boron-doped diamond and Pt anodes, J. Electroanal. Chem. 627 (2009) 41–50.
[21] J. Rodriguez, M.A. Rodrigo, M. Panizza, G. Cerisola, Electrochemical oxidation of Acid Yellow 1 using diamond anode, J. Appl. Electrochem. 39 (2009) 2285–2289.
[22] S. Yoshihara, M. Murugananthan, Decomposition of various endocrine-disrupting chemicals at boron-doped diamond electrode, Electrochim. Acta 54 (2009) 2031–2038.
[23] J. Boudreau, D. Bejan, S. Li, N.J. Bunce, Competition between electrochemical advanced oxidation and electrochemical hypochlorination of sulfamethoxazole at a boron-doped diamond anode, Ind. Eng. Chem. Res. 49 (2010) 2537–2542.
[24] M. Panizza, I. Sirés, G. Cerisola, Anodic oxidation of mecoprop herbicide at lead dioxide, J. Appl. Electrochem. 38 (2008) 923–929.
[25] I. Sirés, C.T.J. Low, C. Ponce-de-León, F.C. Walsh, The deposition of nanostructured β-PbO_2 coatings from aqueous methanesulfonic acid for the electrochemical oxidation of organic pollutants, Electrochem. Commun. 12 (2010) 70–74.
[26] D. Pavlov, B. Monahov, Mechanism of the elementary electrochemical processes taking place during oxygen evolution on the lead dioxide electrode, J. Electrochem. Soc. 143 (1996) 3616–3629.
[27] A. Kapalka, G. Fóti, C. Comninellis, The importance of electrode material in environmental electrochemistry. Formation and reactivity of free hydroxyl radicals on boron-doped diamond electrodes, Electrochim. Acta 54 (2009) 2018–2023.
[28] A. Sánchez-Carretero, C. Sáez, P. Cañizares, M.A. Rodrigo, Electrochemical production of perchlorates using conductive diamond electrolyses, Chem. Eng. J. 166 (2011) 710–714.
[29] G.R. Agladze, G.S. Tsurtsumia, B.-I. Jung, J.-S. Kim, G. Gorelishvili, Comparative study of chemical and electrochemical Fenton treatment of organic pollutants in wastewater, J. Appl. Electrochem. 37 (2007) 985–990.
[30] S. Hammami, N. Oturan, N. Bellakhal, M. Dachraoui, M.A. Oturan, Oxidative degradation of direct Orange 61 by electro-Fenton process using a carbon felt electrode: application of the experimental design methodology, J. Electroanal. Chem. 610 (2007) 75–84.
[31] J.M. Peralta-Hernández, Y. Meas-Vong, F.J. Rodríguez, T.W. Chapman, M.I. Maldonado, L.A. Godínez, Comparison of hydrogen peroxide-based processes for treating dye-containing wastewater: decolorization and destruction of Orange II azo dye in dilute solution, Dyes Pigments 76 (2008) 656–662.
[32] S. Figueroa, L. Vázquez, A. Alvarez-Gallegos, Decolorizing textile wastewater with Fenton's reagent electrogenerated with a solar photovoltaic cell, Water Res. 43 (2009) 283–294.
[33] A. Özcan, M.A. Oturan, N. Oturan, Y. Şahin, Removal of Acid Orange 7 from water by electrochemically generated Fenton's reagent, J. Hazard. Mater. 163 (2009) 1213–1220.
[34] M. Panizza, G. Cerisola, Electro-Fenton degradation of dyes, Water Res. 43 (2009) 339–344.
[35] E. Rosales, M. Pazos, M.A. Longo, M.A. Sanromán, Electro-Fenton decoloration of dyes in a continuous reactor: a promising technology in colored wastewater treatment, Chem. Eng. J. 155 (2009) 62–67.
[36] A.R. Khataee, V. Vatanpour, A.R. Amani Ghadim, Decolorization of C.I. Acid Blue 9 solution by UV/Nano-TiO_2, Fenton, Fenton-like, electro-Fenton and electrocoagulation processes: a comparative study, J. Hazard Mater. 161 (2010) 1225–1233.
[37] N. Oturan, M.A. Oturan, Degradation of three pesticides used in viticulture by electrogenerated Fenton's reagent, Agron. Sustain. Dev. 25 (2005) 267–270.
[38] A. Kesraoui Abdessalem, N. Oturan, N. Bellakhal, M. Dachraoui, M.A. Oturan, Experimental design methodology applied to electro-Fenton treatment for degradation of herbicide chlortoluron, Appl. Catal. B-Environ. 78 (2007) 334–341.
[39] I. Sirés, F. Centellas, J.A. Garrido, R.M. Rodríguez, C. Arias, P.L. Cabot, E. Brillas, Mineralization of clofibric acid by electrochemical advanced oxidation processes using a boron-doped diamond anode and Fe^{2+} and UVA light as catalysts, Appl. Catal. B-Environ. 72 (2007) 373–381.
[40] M. Skoumal, R.M. Rodríguez, P.L. Cabot, F. Centellas, J.A. Garrido, C. Arias, E. Brillas, Electro-Fenton, UVA photoelectro-Fenton and solar photoelectro-Fenton degradation of the drug ibuprofen in acid aqueous medium using platinum and boron-doped diamond anodes, Electrochim. Acta 54 (2009) 2077–2085.
[41] A. Dirany, I. Sirés, N. Oturan, M.A. Oturan, Electrochemical abatement of the antibiotic sulfamethoxazole from water, Chemosphere 81 (2010) 594–602.
[42] I. Sirés, N. Oturan, M.A. Oturan, Electrochemical degradation of β-blockers. Studies on single and multicomponent synthetic aqueous solutions, Water Res. 44 (2010) 3109–3120.
[43] E. Isarain-Chávez, P.L. Cabot, F. Centellas, R.M. Rodríguez, C. Arias, J.A. Garrido, E. Brillas, Electro-Fenton and photoelectro-Fenton degradations of the drug beta-blocker propranolol using a Pt anode: identification and evolution of oxidation products, J. Hazard. Mater. 185 (2011) 1228–1235.
[44] E. Brillas, M.A. Baños, S. Camps, C. Arias, P.L. Cabot, J.A. Garrido, R.M. Rodríguez, Catalytic effect of Fe^{2+}, Cu^{2+} and UVA light on the electrochemical degradation of nitrobenzene using an oxygen-diffusion cathode, New J. Chem. 28 (2004) 314–322.
[45] D. Montanaro, E. Petrucci, C. Merli, Anodic, cathodic and combined treatments for the electrochemical oxidation of an effluent from the flame retardant industry, J. Appl. Electrochem. 38 (2008) 947–954.
[46] M. Yoshida, B.D. Lee, M. Hosomi, Decomposition of aqueous tetrachloroethylene by Fenton oxidation treatment, Water Sci. Technol. 42 (2000) 203–208.
[47] Z. Qiang, W. Ben, C.-P. Huang, Fenton process for degradation of selected chlorinated aliphatic hydrocarbons exemplified by trichloroethylene, 1,1-dichloroethylene and chloroform, Front. Environ. Sci. Eng. China 2 (2008) 397–407.
[48] M. Vilve, S. Vilhunen, M. Vepsäläinen, T.A. Kurniawan, N. Lehtonen, H. Isomäki, M. Sillanpää, Degradation of 1,2-dichloroethane from wash water of ion-exchange resin Fenton's oxidation, Environ. Sci. Pollut. Res. 17 (2010) 875–884.
[49] P. Pichat, L. Cermenati, A. Albini, D. Mas, H. Delprat, C. Guillard, Degradation processes of organic compounds over UV-irradiated TiO_2. Effect of ozone, Res. Chem. Intermed. 26 (2000) 161–170.
[50] S. Malato Rodríguez, J. Blanco Gálvez, M.I. Maldonado Rubio, P. Fernández Ibáñez, W. Gernjak, I. Oller Alberola, Treatment of chlorinated solvents by TiO_2 photocatalysis and photo-Fenton: influence of operating conditions in a solar pilot plant, Chemosphere 58 (2005) 391–398.
[51] R.F.P. Nogueira, M.R.A. Silva, A.G. Trovo, Influence of the iron source on the solar photo-Fenton degradation of different classes of organic compounds, Solar Energy 79 (2005) 384–392.
[52] W.-S. Lee, J.-E. Kim, H.-S. Kim, C.-Y. Ahn, H.-M. Oh, Serial degradation of perchloroethylene by Delftia sp. N6 after dechlorination using Fenton's reagent, J. Microbiol. Biotechnol. 16 (2006) 1734–1739.
[53] J. Marugán, J. Aguado, W. Gernjak, S. Malato, Solar photocatalytic degradation of dichloroacetic acid with silica-supported titania at pilot plant scale, Catal. Today 129 (2007) 59–68.
[54] O. Scialdone, C. Guarisco, A. Galia, R. Herbois, Electroreduction of aliphatic chlorides at silver cathodes in water, J. Electroanal. Chem. 641 (2010) 14–22.
[55] R. Bejankiwar, J.A. Lalman, R. Seth, N. Biswas, Electrochemical degradation of 1,2-dichloroethane (DCA) in a synthetic groundwater medium using stainless-steel electrodes, Water Res. 39 (2005) 4715–4724.
[56] O. Scialdone, A. Galia, G. Filardo, Electrochemical incineration of 1,2-dichloroethane: effect of the electrode material, Electrochim. Acta 53 (2008) 7220–7225.
[57] O. Scialdone, A. Galia, L. Gurreri, S. Randazzo, Electrochemical abatement of chloroethanes in water: reduction, oxidation and combined processes, Electrochim. Acta 55 (2010) 701–708.

[58] I. Sirés, P.L. Cabot, F. Centellas, J.A. Garrido, R.M. Rodríguez, C. Arias, E. Brillas, Electrochemical degradation of clofibric acid in water by anodic oxidation. Comparative study with platinum and boron-doped diamond electrodes, Electrochim. Acta 52 (2006) 75–85.
[59] S. Ferro, A. De Battisti, I. Duo, C. Comninellis, W. Haenni, A. Perret, Chlorine evolution at highly boron-doped diamond electrodes, J. Electrochem. Soc. 147 (2000) 2614–2619.
[60] M. Murata, T.A. Ivandini, M. Shibata, S. Nomura, A. Fujishima, Y. Einaga, Electrochemical detection of free chlorine at high boron-doped diamond electrodes, J. Electroanal. Chem. 612 (2008) 29–36.
[61] A.M. Polcaro, A. Vacca, M. Mascia, S. Palmas, J. Rodriguez Ruiz, Electrochemical treatment of waters with BDD anodes: kinetics of the reactions involving chlorides, J. Appl. Electrochem. 39 (2009) 2083–2092.
[62] M. Mascia, A. Vacca, A.M. Polcaro, S. Palmas, J. Rodriguez Ruiz, A. Da Pozzo, Electrochemical treatment of phenolic waters in presence of chloride with boron-doped diamond (BDD) anodes: experimental study and mathematical model, J. Hazard. Mater. 174 (2010) 314–322.
[63] M.E.H. Bergmann, J. Rollin, T. Iourtchouk, The occurrence of perchlorate during drinking water electrolysis using BDD anodes, Electrochim. Acta 54 (2009) 2102–2107.
[64] L.J.J. Janssen, P.D.L. Heyden, Mechanism of anodic oxidation of chlorate to perchlorate on platinum electrodes, J. Appl. Electrochem. 25 (1995) 126–136.
[65] O. Scialdone, A. Galia, C. Guarisco, S. Randazzo, G. Filardo, Electrochemical incineration of oxalic acid at boron doped diamond anodes: role of operative parameters, Electrochim. Acta 53 (2008) 2095–2108.
[66] O. Scialdone, S. Randazzo, A. Galia, G. Silvestri, Electrochemical oxidation of organics in water: role of operative parameters in the absence and in the presence of NaCl, Water Res. 43 (2009) 2260–2272.
[67] S. Ferro, C.A. Martínez-Huitle, A. De Battisti, Electroxidation of oxalic acid at different electrode materials, J. Appl. Electrochem. 40 (2010) 1779–1787.
[68] M.A. Oturan, M. Pimentel, N. Oturan, I. Sirés, Reaction sequence for the mineralization of the short-chain carboxylic acids usually formed upon cleavage of aromatics during electrochemical Fenton treatment, Electrochim. Acta 54 (2008) 173–182.
[69] A. Kapalka, G. Fóti, C. Comninellis, Investigation of the anodic oxidation of acetic acid on boron-doped diamond electrodes, J. Electrochem. Soc. 155 (2008) E27–E32.